Mechatronics 24 (2014) 1242–1253

Contents lists available at ScienceDirect

Mechatronics

journal homepage: www.elsevier.com/locate/mechatronics

Active control of a seat suspension with the system adaptation to varying load mass

I. Maciejewski *, S. Glowinski, T. Krzyzynski

Koszalin University of Technology, Institute of Technology and Education, Division of Mechatronics and Applied Mechanics, Sniadeckich 2, Koszalin 75-453, Poland

ARTICLE INFO

Article history:
Received 28 November 2013
Accepted 26 October 2014
Available online 15 November 2014

Keywords:
Active seat suspension
Vibration damping
Adaptive control

ABSTRACT

This paper deals with the control system design of active seat suspension. The proposed control system structure is built basing on several various controllers. The primary controller is used to evaluate the actual value of the desired active force that should be generated in the suspension system. The secondary controller is employed to calculate the instantaneous value of a signal which controls the active element by means of its reverse model. The adaptation mechanism recognises the actual suspended mass in order to increase the effectiveness of vibration isolation. Additionally, the system robustness for different load masses is investigated using computer simulation and experimental research.

1. Introduction

The amplification of low frequency vibrations occurring in passive seats can be overcome with an active suspension mechanism. The mechanisms of this type employ a source of power to move the seat relative to its base. As the vehicle oscillates, the seat can be held relatively stationary in space under the control of an servo-mechanism. The studies of this problem have been of academic and industrial interest for a long time. At first, the passive suspensions have been investigated [1,2] and afterwards the semi-active [3] and active [4–6] systems have been developed. The conclusion drawn from these articles is that the semi-active and active suspensions enhance comfort considerably when compared to the passive systems. The concept of the semi-active and active suspensions can be successfully applied in road-vehicle suspensions, cabin suspensions in trucks or seat suspensions [7,8]. The main idea of these system is to use suspension control techniques for reducing the vibrations.

According to [9] the semi-active suspension system can be effectively applied to the passenger vehicle with improved both ride comfort and steering stability. Authors tested a car installed with four electro-rheological dampers which allowed to evaluate performance characteristics of the semi-active suspension system associated with skyhook controller. A three-dimensional vehicle model and the general seat suspension model was analysed using optimal dampers in the case of passive, semi-active and active vehicle suspensions [10]. Authors analysed the effects of vibrations and seat positions on comfort and road holding capabilities of 3-D road vehicles as observed in the variation of different parameters such as suspension coefficients, road disturbances and the seat position. By developing an objective function they generated an optimisation algorithm allowing calculation of the optimal suspension parameters. The optimal active suspension of the seat also has been obtained analytically for a human body represented alternatively by apparent mass weighted by standard frequency domain curves depicting discomfort levels [11].

The feedback control is intended to improve the dynamics of suspension systems, especially for a specific working conditions. The control element in semi-active and active vibration isolation systems is adjusted by means of the controller which uses information concerning the system states. However, there are some principal factors that influence the problem of vibration isolation of a whole body system. One of these problems is the selection of the appropriate model parameter like the damping and the stiffness and the problem of H-inf control for the active seat suspension systems via dynamic output feedback control [12]. In the paper [13] static-output-feedback controller design problem is investigated. The two-stage method is developed to determine the static-output-feedback gain matrix for the structural system even if actuator faults occur.

There are some works presented in the existing literature wherein active suspension systems are considered in relation to varying mass loading. A load-dependent controller design approach to solve the problem of the multi-objective control for active suspension systems is presented in the paper [14]. The paper

* Corresponding author.
E-mail addresses: igor.maciejewski@tu.koszalin.pl (I. Maciejewski), sebastian.glowinski@tu.koszalin.pl (S. Glowinski), tomasz.krzyzynski@tu.koszalin.pl (T. Krzyzynski).

http://dx.doi.org/10.1016/j.mechatronics.2014.10.008
0957-4158/

Nomenclature

A_I	effective cross section area of the inlet valve, m^2
A_E	effective cross section area of the outlet valve, m^2
A_{ef}	effective area of the pneumatic spring, m^2
$a_{a1}, a_{a2}, b_{a1}, b_{a2}$	coefficients of logarithmic functions
a_s, b_s, c_s, d_s	coefficients of a cubic equation
F_a	desired active force, N
F_s	force of the pneumatic spring, N
SEAT	Seat Effective Amplitude Transmissibility factor
g	gravity constant, m/s^2
K_{a1}	proportional gain of the relative displacement feedback loop, V/m
K_{a2}	proportional gain of the velocity feedback loop, Vs/m
k_I	static gain of the inlet valve, m^2/V
k_E	static gain of the outlet valve, m^2/V
l_s	variable length the pneumatic spring, m
m	mass of the isolated body, kg
$\dot{m}_I$	mass flow rate for inflating of the pneumatic spring, kg/s
$\dot{m}_E$	mass flow rate for exhausting of the pneumatic spring, kg/s
p_a	atmospheric pressure, Pa
p_s	air pressure inside the pneumatic spring, Pa
p_{s0}	initial pressure of the pneumatic spring, Pa
p_z	air pressure of the power supply, Pa
R	gas constant, J/(kg K)
T	air temperature, K
t	computation time instant, s
t_I	actuating time of the inlet valve, s
t_E	actuating time of the outlet valve, s
u_I	control voltage of the inlet valve, V
u_E	control voltage of the outlet valve, V
u_{max}	maximum value of the control voltage, V
V_s	volume of the pneumatic spring, m^3
x	displacement of the isolated body, m
x_s	displacement of the excitation, m
$(x-x_s)_c$	constraint value imposed on the suspension travel, m
$(x-x_s)_{max}$	suspension travel, m
$(\ddot{x}_w)_{RMS}$	frequency weighted root mean square value of the simulated input acceleration, m/s^2
$(\ddot{x}_{sw})_{RMS}$	frequency weighted root mean square value of the measured seat acceleration, m/s^2
α	parameter of the Mietluk–Awtuszko function
δ_s	reduction ratio of active force acting in the vertical direction on the isolated body
κ	adiabatic coefficient

[15] shows an adaptive sliding controller for a non-autonomous suspension system with time-varying loadings. However, the usefulness and the advantages of the proposed controller design methodology are demonstrated via numerical simulations only. The objective of this paper is to suggest a new control strategy in order to increase vibro-isolating properties of the active seat suspension in response to varying load mass. In the paper [16], the first simulation results have been discussed, while the presented adaptive control is investigated experimentally using a laboratory method for measuring and evaluating the effectiveness of the seat suspension in reducing the vertical whole-body vibration.

The contribution of the paper consists in a better vibration control of seat suspension and a higher system robustness to the operator's mass variations. Using a unique vibration control system, that structure and individual components are presented in this paper, it is possible to achieve the desired system properties in view of the different requirements for the modern seat suspension systems.

2. Simulated input vibration to evaluate the SEAT factor and suspension travel

The International Standard [17] specifies the input vibrations for the purpose of determining the Seat Effective Amplitude Transmissibility (SEAT) factor [18]. The particular input vibration is used to evaluate the seat performance for the different types of earth-moving machinery. Each class (EM1–EM9) defines a group of machine having similar vibration characteristics. In this paper, only selected input vibrations are used to evaluate the seat suspension dynamic behaviour:

- EM3 – an excitation signal representative of wheel loaders.
- EM5 – an excitation signal representative of wheel dozers.
- EM6 – an excitation signal representative of crawler loaders and crawler dozers.

The power spectral densities of mentioned excitation signals are presented in Fig. 1. As shown in this figure, the magnitude of the generated input vibrations has to be within the tolerance of the target power spectral density function, that is defined in the paper [17].

The SEAT factor provides the first numerical assessment of the seat isolation efficiency and its value is calculated as follows [18]:

$$\mathrm{SEAT} = \frac{(\ddot{x}_w)_{RMS}}{(\ddot{x}_{sw})_{RMS}} \tag{1}$$

where $\ddot{x}_{sw}$ is the frequency weighted root mean square value of the simulated input acceleration, $\ddot{x}_w$ is the frequency weighted root mean square value of the measured seat acceleration. The frequency weighting of acceleration signal shall be done in accordance with [19].

The SEAT factor value of 1 means that seating on the floor plate in the working machine cabin would produce the same vibration discomfort. If the SEAT factor value is greater than 1, the vibration discomfort is increased by the seat. If the SEAT factor value is less than 1, the useful vibro-isolation is provided by the seat.

The second numerical assessment of the seat dynamic performance is the suspension travel $(x-x_s)_{max}$. In this paper, the suspension travel is defined by the maximum relative displacement of suspension system and its value is calculated as follows [20]:

$$(x-x_s)_{max} = \max_t(x-x_s) - \min_t(x-x_s) \tag{2}$$

where x is the displacement of the seat and x_s is the displacement of the input vibration, t is the computation time instant.

There is no comfort criteria standards for the selection of the trade-off between the SEAT factor and the suspension travel $(x-x_s)_{max}$. On the one hand the SEAT factor should be minimised, but this is only the first objective of a system evaluation. The second objective is that the suspension travel has to be small in order to ensure, that even very rough road profiles do not cause the deflection limits to be reached [21]. An improvement in one objective requires a degradation of another, therefore these objectives conflict. Consequently, the design of seat suspension systems can be treated as an optimisation problem.

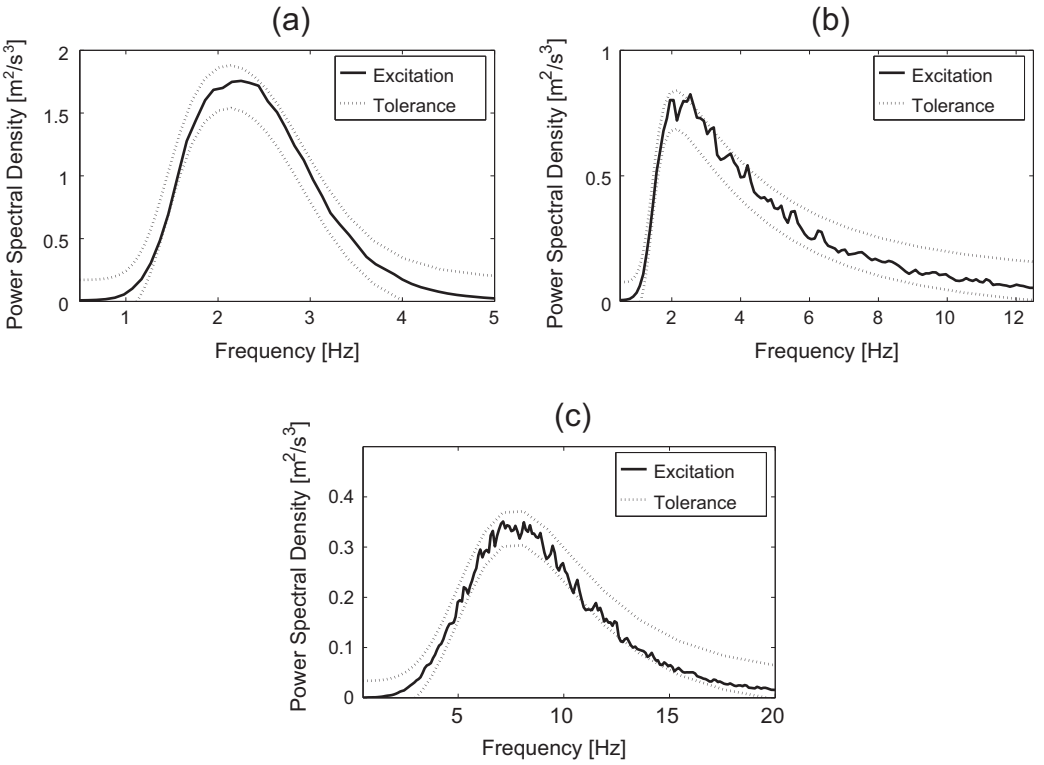

Fig. 1. Power spectral densities of the excitation signal for various spectral classes: EM3 (a), EM5 (b), EM6 (c) and their tolerances defined in ISO 7096 [17].

There are two performance indices introduced to evaluate the suspension performance, i.e. the SEAT factor (Eq. (1)) and a limitation on the relative displacement (Eq. (2)). The same limitation exists on the force actuator, which must be lower than the maximum actuator force to avoid performance reduction. However, this limitation is strictly connected with the available capacity of the specific force actuator applied to the active system. Therefore, in the following paper the control signal sent to the force actuator is constrained within the operating range (Eq. (13)).

3. Active seat suspension for earth-moving machinery

The operators of the earth-moving machinery are very often exposed to a low frequency vibration. Such a situation is very unfavourable and leads to the loss of the concentration, tiredness and decrease of the effectiveness of the work being performed. In the case of typical working machines without flexible wheel suspension, a seat suspension is the only system that can protect the operator against vibration. Most often, the passive seat suspension amplifies the vibration amplitudes at resonance frequencies that results in cutting down their working time. For this reason seating systems are constantly improved in order to eliminate vibration and increase the operator ride comfort [7,10–12].

The investigated seat suspension is an exemplary one (Fig. 2), that is representative for the isolation of low frequency vibration at medium amplitudes. This kind of vibration isolators are used for seats in the earth moving-machinery. In order to improve a ride comfort, it is important to keep the acceleration of isolated body small over the frequency range of excitation signal (aimed to protect a human operator against vibration). At the same time, it is important to keep a relative displacement of suspension system small.

The considered seat suspension system consists of a shear-guidance mechanism, a pneumatic spring and a hydraulic shock-absorber (Fig. 2). The active system uses the air-flow (inflating $\dot{m}_I$ and exhausting $\dot{m}_E$) that is regulated by means of two proportional valves and the control signals u_I and u_E. Inflating the pneumatic spring is carried out by an external air compressor and the exhaust of the pneumatic spring is released directly to the atmosphere. The air-flow changes the air pressure inside the air-spring and the variation of pressure creates an active force for the suspension system. The equation of motion of this seat suspension has been explored in the authors' previous papers [20,22]. Moreover, in those papers the mathematical models of the basic forces in the system, i.e. the spring force, the damping force, the forces from end-stop buffers, the overall friction force of suspension system and the gravity force of isolated body, have been modelled and verified experimentally.

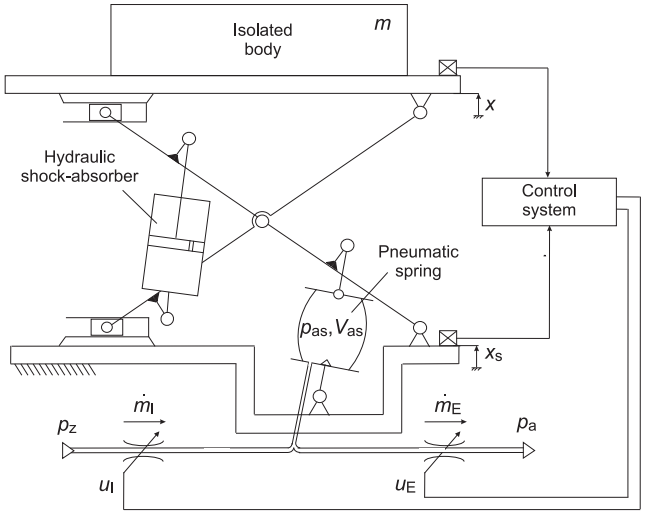

Fig. 2. Active seat suspension system.

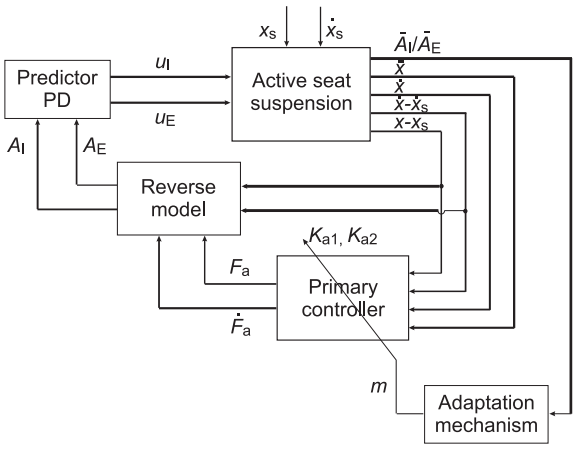

Fig. 3. Proposed control system of the active seat suspension with an adaptation mechanizm to varying load mass.

4. Control system design of the active seat suspension

The block diagram of proposed control system of the active seat suspension is presented in Fig. 3. In this control system, the desired active force $(F_a, \dot{F}_a)$ is calculated using the primary controller. If the desired force is evaluated, then this force should be reproduced by the active element applied in the seat suspension. Therefore the actual effective areas (A_I, A_E) of proportional control valves are calculated using reverse model of the pneumatic spring. Due to the speeding up the control signals (u_I, u_E) by the PD predictor, the actuating time of the force actuator is eliminated. In addition, an adaptation mechanism evaluates the controller settings (K_{a1}, K_{a2}) as a function of the suspended mass (m). This mass is recognised based on the mean values over time of the effective cross section areas of inlet and outlet valves $(\bar{A}_I, \bar{A}_E)$. A detailed description of the each control system components is presented in the next subsections.

4.1. Primary controller

A simplified model of the hybrid suspension is used to determine the desired force F_a that should be introduced into the system actively (Fig. 4a). Subsequently, this desired force should be reproduced by the pneumatic spring that is inflated or exhausted in order to generate the force F_s (Fig. 4b).

The relationships for the desired active force and its time derivative can be formulated in the following form [7]:

$$F_a = K_{a1}(x - x_s) + K_{a2}\dot{x} \tag{3}$$

$$\dot{F}_a = K_{a1}(\dot{x} - \dot{x}_s) + K_{a2}\ddot{x} \tag{4}$$

where $x - x_s$ is the relative displacement of suspension system, $\dot{x}$ is the velocity of suspended mass, $\dot{x} - \dot{x}_s$ is the relative velocity of suspension system, $\ddot{x}$ is the acceleration of body acceleration, K_{a1} and K_{a2} are the primary controller settings to be designed.

The desired active force described by Eq. (3) is applied to control the dynamic behaviour of seat suspension system. The proportional part $K_{a1}(x - x_s)$ of this function allows to reduce the relative motion between the suspended body and the seat base. The derivative part $K_{a2}\dot{x}$ is a function of the absolute motion used in order to attenuate the vibration transmitted to the isolated body. This strategy of improving seat suspension vibro-isolation properties contributes to better health protection of the operator while maintaining the controllability of the working machine.

4.2. Simplified model of the pneumatic spring

A simplified model of the pneumatic spring relies on the isothermal behaviour of the air. According to this model, the actual value of air pressure p_s inside the pneumatic spring is defined as [23]:

$$\dot{p}_s = \frac{1}{V_s}\left(RT(\dot{m}_I - \dot{m}_E) - p_s\dot{V}_s\right) \tag{5}$$

where V_s is the variable volume of the pneumatic spring, R is the gas constant, T is the air temperature. Defining pressure–force relation of the pneumatic spring $p_s = F_s/A_{ef} + p_{s0}$ and its variable volume $V_s = A_{ef}l_s$, the force of the pneumatic spring can be calculated as follows:

$$\dot{F}_s = \frac{1}{l_s}\left(RT(\dot{m}_I - \dot{m}_E) - (F_s + A_{ef}p_{s0})\dot{l}_s\right) \tag{6}$$

where l_s is the variable length of the pneumatic spring, A_{ef} is the effective area of the pneumatic spring, p_{s0} is the initial pressure of the pneumatic spring.

The mass flow rates $\dot{m}_I$ and $\dot{m}_E$ are calculated using the Mietluk–Awtuszko function [24] as follows:

- for inflating of the pneumatic spring

$$\dot{m}_I = 0.5787A_I p_z\sqrt{\kappa}\sqrt{\frac{1}{RT}}\alpha\frac{1 - \left(\frac{F_s}{A_{ef}} + p_{s0}\right)\Big/p_z}{\alpha - \left(\frac{F_s}{A_{ef}} + p_{s0}\right)\Big/p_z} \tag{7}$$

- for exhausting of the pneumatic spring

$$\dot{m}_E = 0.5787A_E\left(\frac{F_s}{A_{ef}} + p_{s0}\right)\sqrt{\kappa}\sqrt{\frac{1}{RT}}\alpha\frac{1 - p_a\Big/\left(\frac{F_s}{A_{ef}} + p_{s0}\right)}{\alpha - p_a\Big/\left(\frac{F_s}{A_{ef}} + p_{s0}\right)} \tag{8}$$

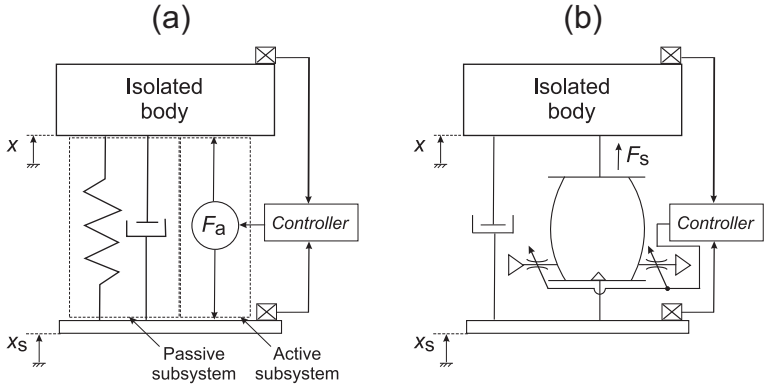

Fig. 4. Simplified models of the active seat suspensions: with the force actuator (a), with the pneumatic spring (b).

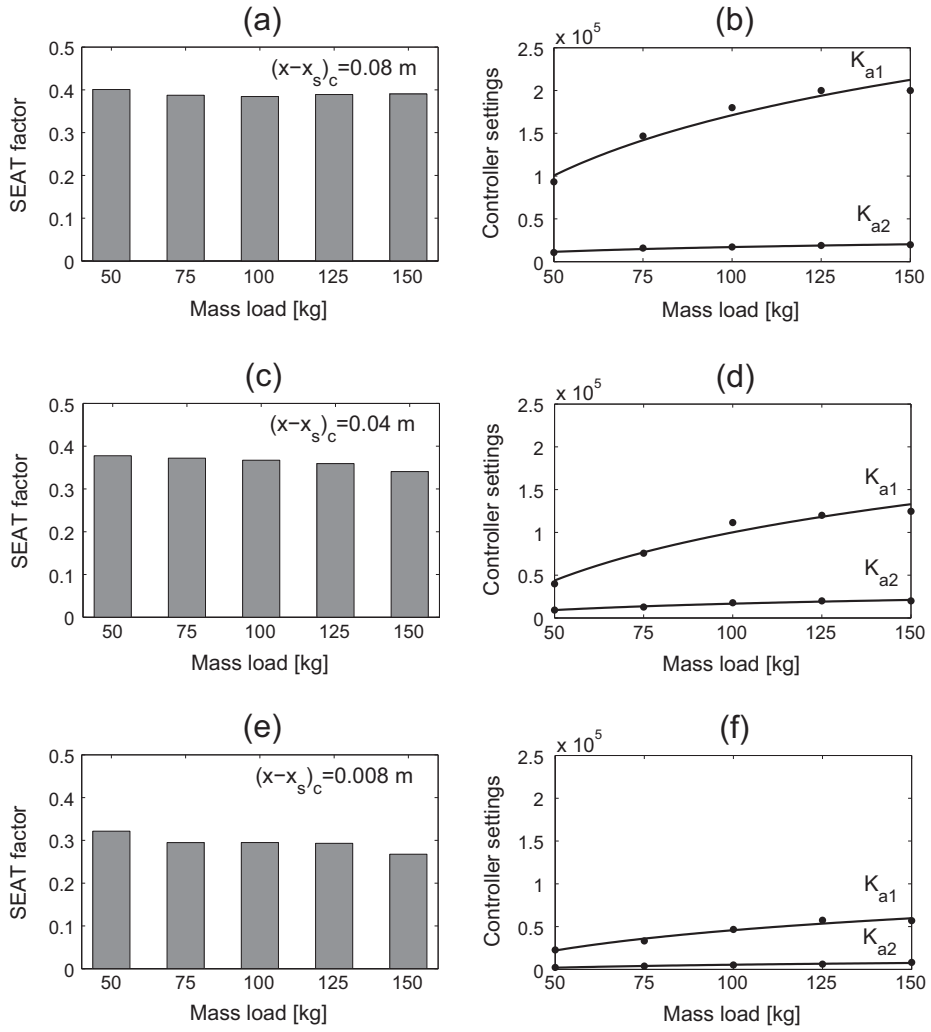

Fig. 5. Optimisation results for various spectral classes of the excitation signal: EM3 (a) and (b), EM5 (c) and (d), EM6 (e) and (f) obtained at different constraints $(x - x_s)_c$ imposed on suspension travel.

where A_I is the effective cross section area of inlet valve, A_E is the effective cross section area of outlet valve, p_z is the air pressure of power supply, p_a is the atmospheric pressure, κ is the adiabatic coefficient, α is the parameter of the Mietluk–Awtuszko function.

4.3. Reverse model of the pneumatic spring

The description of the pneumatic spring force relating to the mass flow rate (Eq. (5)) can be rearranged in the following form:

$$\dot{m}_I - \dot{m}_E = \frac{1}{RT}\left(\frac{l_s}{\delta_s}\dot{F}_a + \left(\frac{F_a}{\delta_s} + A_{ef}p_{s0}\right)\dot{l}_s\right) \tag{9}$$

where $\dot{m}_I - \dot{m}_E$ is the mass flow rate to achieve desired active force, δ_s is the reduction ratio of active force acting in the vertical direction on the isolated body, F_a and $\dot{F}_a$ are the desired active force and its first derivative over the time.

The Mietluk–Awtuszko functions (Eqs. (7) and (8)) has to be rearranged in order to obtain such mass flow rate (Eq. (9)). According to this function, the effective cross section area of the inlet valve should varied as follows:

$$A_I = \frac{\dot{m}_I}{0.5787 p_z \sqrt{\kappa}\sqrt{\frac{1}{RT}}\alpha \frac{1-\left(\frac{F_a}{\delta_s A_{ef}}+p_{s0}\right)\Big/ p_z}{\alpha-\left(\frac{F_a}{\delta_s A_{ef}}+p_{s0}\right)\Big/ p_s}} \tag{10}$$

$$A_E = \frac{-\dot{m}_E}{0.5787\left(\frac{F_a}{\delta_s A_{ef}}+p_{s0}\right)\sqrt{\kappa}\sqrt{\frac{1}{RT}}\alpha \frac{1-p_a\Big/\left(\frac{F_a}{\delta_s A_{ef}}+p_{s0}\right)}{\alpha-p_a\Big/\left(\frac{F_a}{\delta_s A_{ef}}+p_{s0}\right)}} \tag{11}$$

4.4. Predictor PD

The effective cross section areas A_I and A_E are assumed to be proportional to the electric input signals u_I and u_E when using the directional control valves. Taking into account the actuating times t_I and t_E of the proportional control valves (for inlet and outlet valves, respectively), the electric input signals are subsequently formed by the proportional-derivative (PD) predictor as follows:

$$u_I = \frac{1}{k_I}\left(t_I\dot{A}_I + A_I\right), \quad u_E = \frac{1}{k_E}\left(t_E\dot{A}_E + A_E\right) \tag{12}$$

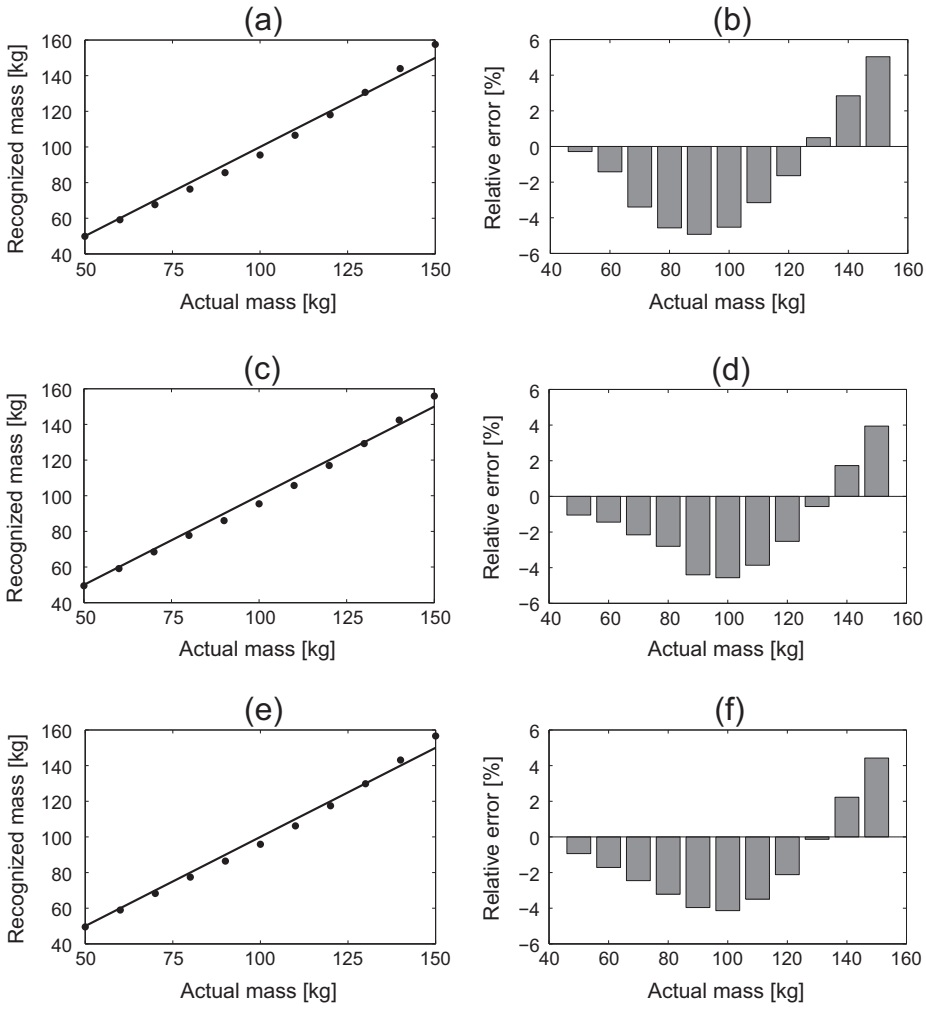

Fig. 6. Recognised mass load as a function of the actual mass load and the corresponding relative error for various spectral classes of the excitation signal: EM3 (a) and (b), EM5 (c) and (d), EM6 (e) and (f).

where k_I is the static gain of the inlet valve and k_E is the static gain of the outlet valve. The electric input signals for the inlet and outlet control valves are finally limited in the operating ranges as:

$$u_I = \begin{cases} 0 & \text{dla } u_I < 0 \\ u_I & \text{dla } 0 \leqslant u_I < u_{max} \\ u_{max} & \text{dla } u_I \geqslant u_{max} \end{cases} \quad u_E = \begin{cases} 0 & \text{dla } u_E < 0 \\ u_E & \text{dla } 0 \leqslant u_E < u_{max} \\ u_{max} & \text{dla } u_E \geqslant u_{max} \end{cases} \tag{13}$$

where u_{max} is the maximum input voltage that is responsible for the complete opening of the proportional flow control valves.

4.5. Optimisation of the primary controller settings

In order to optimise the suspension system vibro-isolating properties for a given excitation signal, the SEAT factor is utilised as the optimisation objective:

$$\min_{K_{a1}, K_{a2}} \text{SEAT}(K_{a1}, K_{a2}) \tag{14}$$

The suspension travel $(x - x_s)_{max}$ is transferred to a nonlinear inequality constraint as follows [7]:

$$(x - x_s)_{max} \leqslant (x - x_s)_c \tag{15}$$

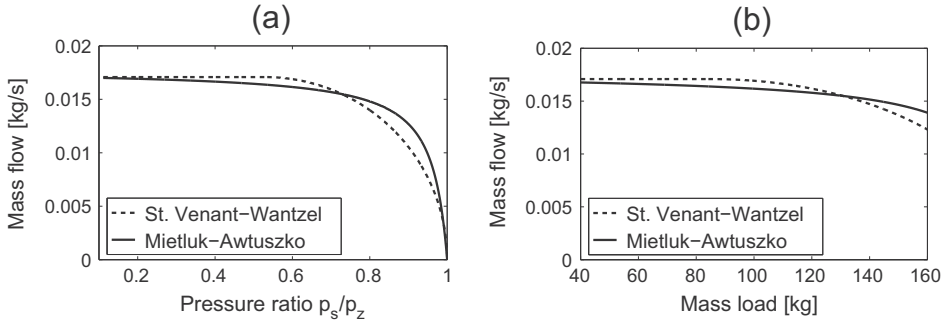

Fig. 7. Mass flow rates as a function of the pressure ratio (a) and the mass load (b) calculated using different models.

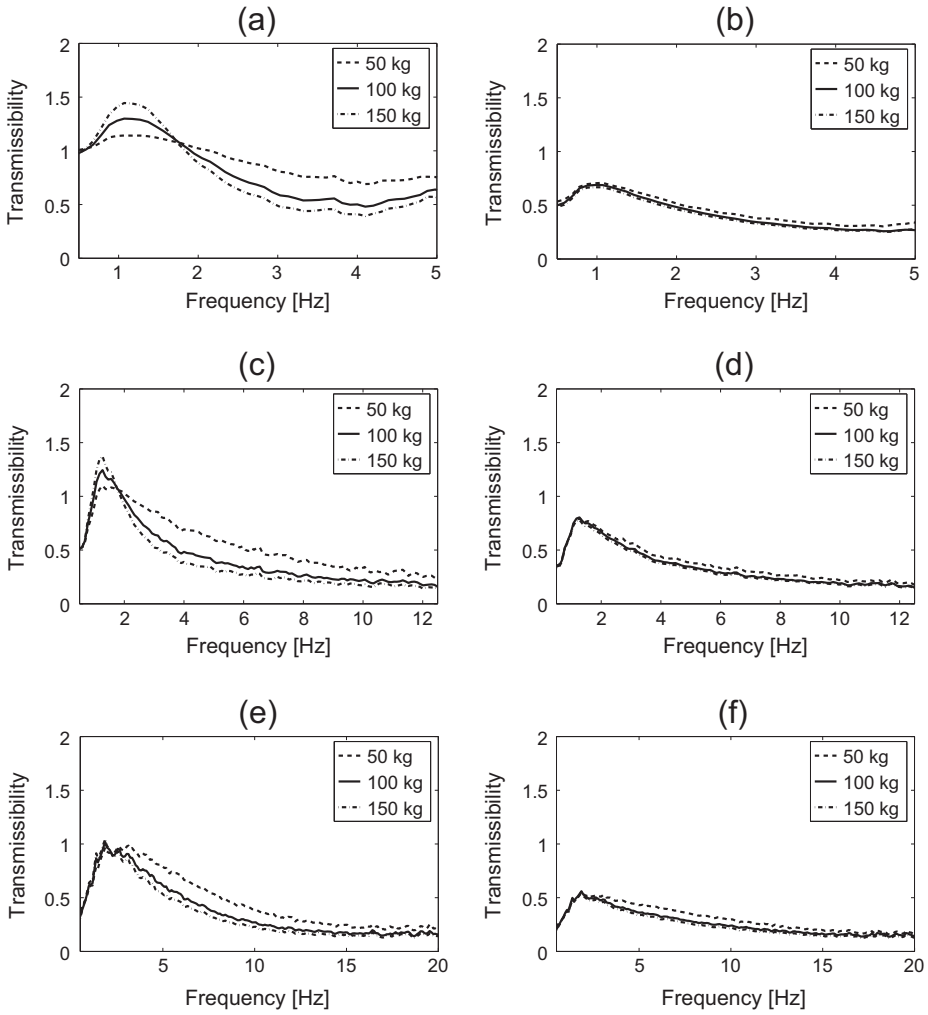

Fig. 8. Simulated transmissibility functions of the passive seat suspension for various spectral classes of the excitation signal: EM3 (a), EM5 (c), EM6 (e) and simulated transmissibility functions of the active seat suspension for various spectral classes of the excitation signal: EM3 (b), EM5 (d), EM6 (f).

where $(x - x_s)_c$ defines the constraint value imposed on the suspension travel. The linear inequality constraints are the following ranges of decision variables (primary controller settings):

- gain factor of the relative displacement feedback loop $K_{a1} = 20\text{–}200 \times 10^3$ N/m,
- gain factor of the absolute velocity feedback loop $K_{a2} = 2\text{–}20 \times 10^3$ Ns/m.

This problem is solved by the optimisation algorithm that attempts to find a constrained minimum of the objective function starting at an initial estimate. The initial starting points of decision variables (K_{a1} and K_{a2}) are generated randomly, ten times for each value of the suspended mass: 50 kg, 75 kg, 100 kg, 125 kg and 150 kg. This procedure has allowed to find the minimum of the SEAT factor and ensures a high probability that the found optimum is a global one. The optimisation results obtained for the selected spectral classes of excitation signal (EM3, EM5 and EM6) are presented in Fig. 5.

The results of the optimisation (Fig. 5a, c, and e) show the possibility of obtaining nearly the same dynamic behaviour of the active seat suspension for different mass load (the SEAT factors are nearly equal for particular excitation signals). In order to achieve such a satisfactory system performance, the controller settings K_{a1} and K_{a2} should be described as a function of the suspended mass m. These dependency are approximated using the logarithmic functions as follows:

$$K_{a1} = a_{a1} \ln(m) + b_{a1} \quad (16)$$

$$K_{a2} = a_{a2} \ln(m) + b_{a2} \quad (17)$$

where a_{a1}, b_{a1} and a_{a2}, b_{a2} are the coefficients of the logarithmic functions to be evaluated by the least square approximation. The

Table 1
Simulation results of the active seat suspension for various spectral classes of the excitation signal and different mass loading.

Excitation signal	Mass load (kg)	Passive		Active	
		SEAT factor	Suspension travel (mm)	SEAT factor	Suspension travel (mm)
EM3	50	0.907	57	0.429	79
	100	0.779	84	0.391	80
	150	0.716	99	0.371	82
EM5	50	0.620	41	0.421	40
	100	0.477	62	0.377	41
	150	0.417	74	0.352	41
EM6	50	0.526	9	0.335	8
	100	0.392	11	0.275	9
	150	0.339	12	0.254	9

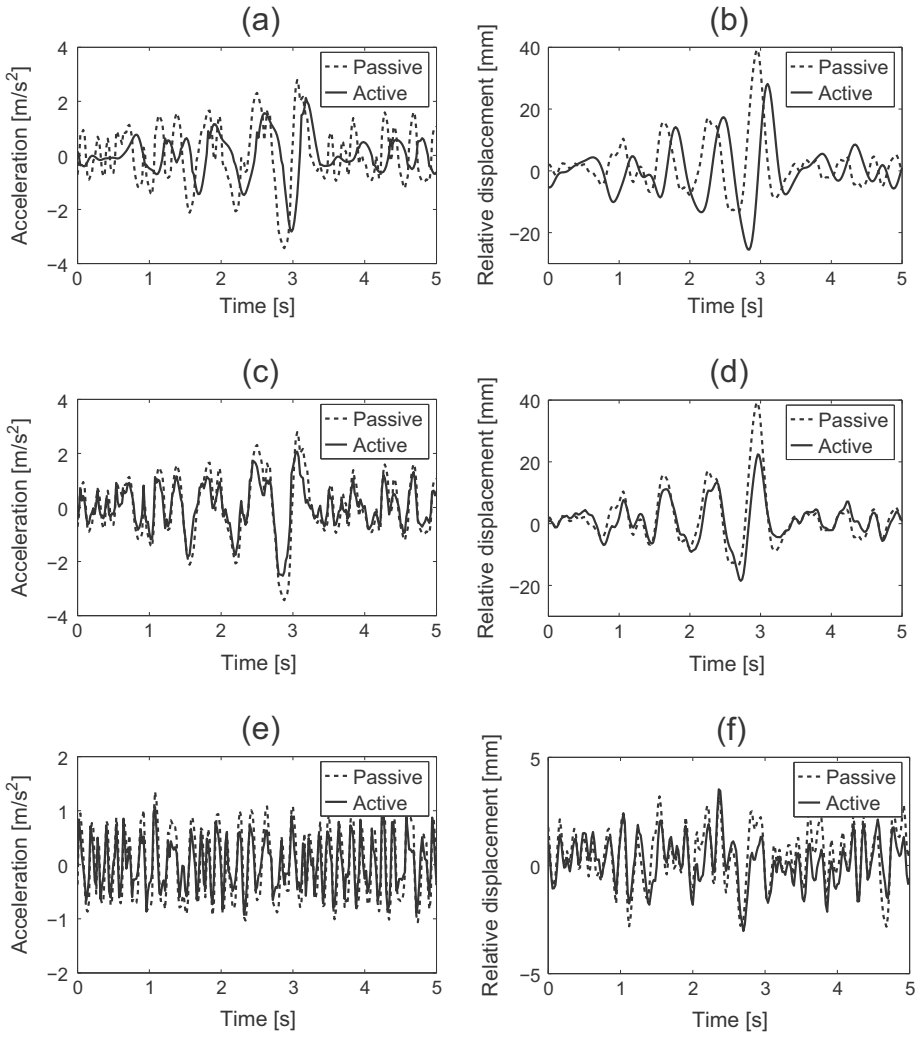

Fig. 9. Simulated accelerations of the suspended body for excitation signals: EM3 (a), EM5 (c), EM6 (e) and relative displacements of the seat suspension for excitation signals: EM3 (b), EM5 (d), EM6 (f), suspended mass 100 kg.

approximation results, that show the dependency of the controller settings: K_{a1} and K_{a2} for different m, are shown in Fig. 5b, d, and f.

4.6. Adaptation mechanism

The load-dependent controller is proposed to control the active suspension system more efficiently. The controller settings K_{a1} and K_{a2} depend on the information of the suspended mass m and its value has to be known. This causes that an additional sensor would be employed in order to recognise the mass load. However, the online available information of the pneumatic spring inflation/deflation can be employed to recognise the actual mass load of the active seat suspension. Using a rule that the mean values of inflated and exhausted air are equal ($\dot{m}_I = \dot{m}_E$), the corresponding Mietluk–Awtuszko functions (Eqs. (7) and (8)) can be compared in the following form:

$$\overline{A}_I p_z \frac{1-\bar{p}_s/p_z}{\alpha-\bar{p}_s/p_z} = \overline{A}_E \bar{p}_s \frac{1-p_a/\bar{p}_s}{\alpha-p_a/\bar{p}_s} \tag{18}$$

where $\bar{p}_s$ is the mean value over time of the pressure inside the pneumatic spring. Defining the relation $\overline{A}_I/\overline{A}_E$ of the effective cross section areas of the inlet and outlet valves, Eq. (15) can be rewritten to the following form:

$$\frac{\overline{A}_I}{\overline{A}_E} = \frac{(\bar{p}_s^2 - p_a\bar{p}_s)(\alpha p_z - \bar{p}_s)}{(\alpha\bar{p}_s - p_a)(p_z^2 - p_z\bar{p}_s)} \tag{19}$$

Setting the above function as $f(\bar{p}_s) = 0$, the following cubic equation can be obtained:

$$a_s\bar{p}_s^3 + b_s\bar{p}_s^2 + c_s\bar{p}_s + d_s = 0 \tag{20}$$

where the coefficients: a_s, b_s, c_s, d_s of a cubic equation are described as follows:

$$\begin{aligned} &a_s = 1 \quad b_s = -\frac{\overline{A}_I}{\overline{A}_E}\alpha p_z - \alpha p_z - p_a \\ &c_s = \frac{\overline{A}_I}{\overline{A}_E}\alpha p_z^2 + \frac{\overline{A}_I}{\overline{A}_E}p_z p_a + \alpha p_z p_a \quad d_s = -\frac{\overline{A}_I}{\overline{A}_E}p_z^2 p_a \end{aligned} \tag{21}$$

Solving the cubic equation (Eq. (20)) amounts to finding the roots of a cubic function. Defining a discriminant of the cubic equation in the form:

$$\Delta = \left(\frac{q}{3}\right)^3 + \left(\frac{r}{2}\right)^2, \quad q = \frac{c_s}{a_s} - \frac{b_s^2}{3a_s^2}, \quad r = \frac{2b_s^3}{27a_s^3} + \frac{d_s}{a_s} - \frac{b_s c_s}{3a_s^2} \tag{22}$$

then for $\Delta < 0$ is possible to find each real roots of the cubic function (Eq. (20)) in the form:

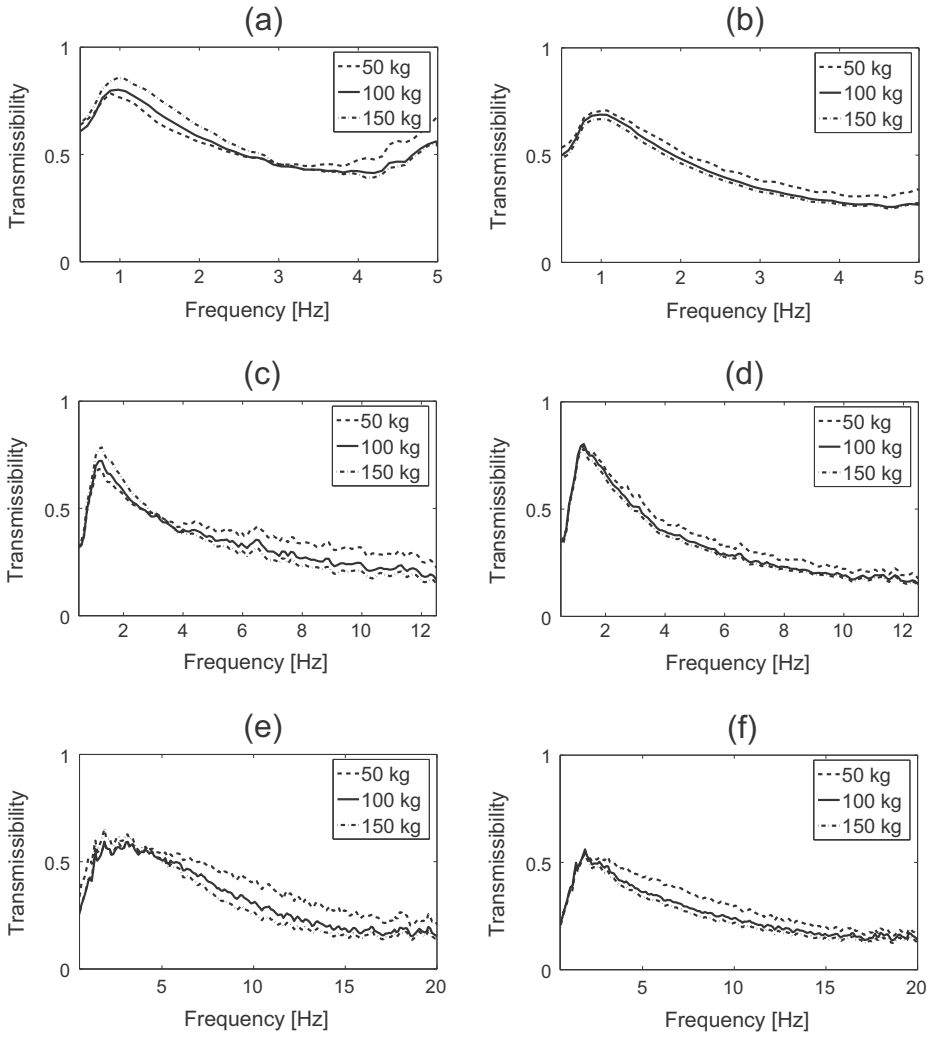

Fig. 10. Simulated transmissibility functions of the active seat suspension with conventional control system for various spectral classes of the excitation signals: EM3 (a), EM5 (c), EM6 (e) and simulated transmissibility functions of the active seat suspension with adaptive mass recognising for various spectral classes of the excitation signals: EM3 (b), EM5 (d), EM6 (f).

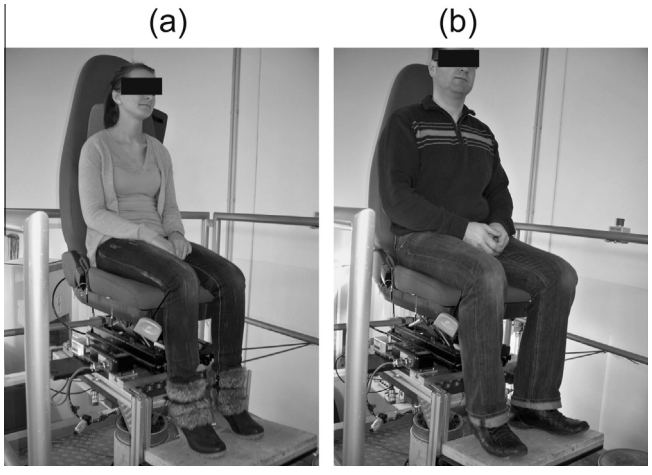

Fig. 11. Test person set-up: the body mass 51 kg (a) and the body mass 102 kg (b).

$$(\bar{p}_s)_i = 2\sqrt{\frac{-q}{2}}\cos\frac{\varphi + 2(i-1)\pi}{3} - \frac{b_s}{3a_s}, \quad \varphi = \arccos\left(\frac{\frac{-r}{2}}{\sqrt{\frac{-q^3}{27}}}\right) \tag{23}$$

where $i = 1, \ldots, 3$ is the number of root found. Then the mass load of active suspension system is calculated for given root number as follows:

$$m = \frac{\delta_s A_{ef}}{g}\left((\bar{p}_s)_i - p_a\right) \tag{24}$$

where g is the gravity constant.

The online calculation of the body mass based on the effective cross section areas of the inlet and outlet valves: $\overline{A}_I$ and $\overline{A}_E$ is enabled using Eqs. (21)–(24). However, the information concerning the actual cross section areas of proportional valves is not easily accessible. Therefore the adaptive load recognising is performed using the control signals: $\bar{u}_I$ and $\bar{u}_I$. In this paper, a quotient of the effective cross section areas of inlet and outlet valves $\overline{A}_I/\overline{A}_E$ is assumed to be approximately equal to a quotient of their control signals multiplied by the corresponding static gains $k_I\bar{u}_I/k_E\bar{u}_E$ (i.e. $\overline{A}_I/\overline{A}_E \approx k_I\bar{u}_I/k_E\bar{u}_E$).

The results of recognised body mass (computation time 300 s) as a function of the actual suspension load, that are obtained for the root number $i = 3$, are presented in Fig. 6a, c, and e. Corresponding relative errors of the recognised mass are shown in Fig. 6b, d, and f.

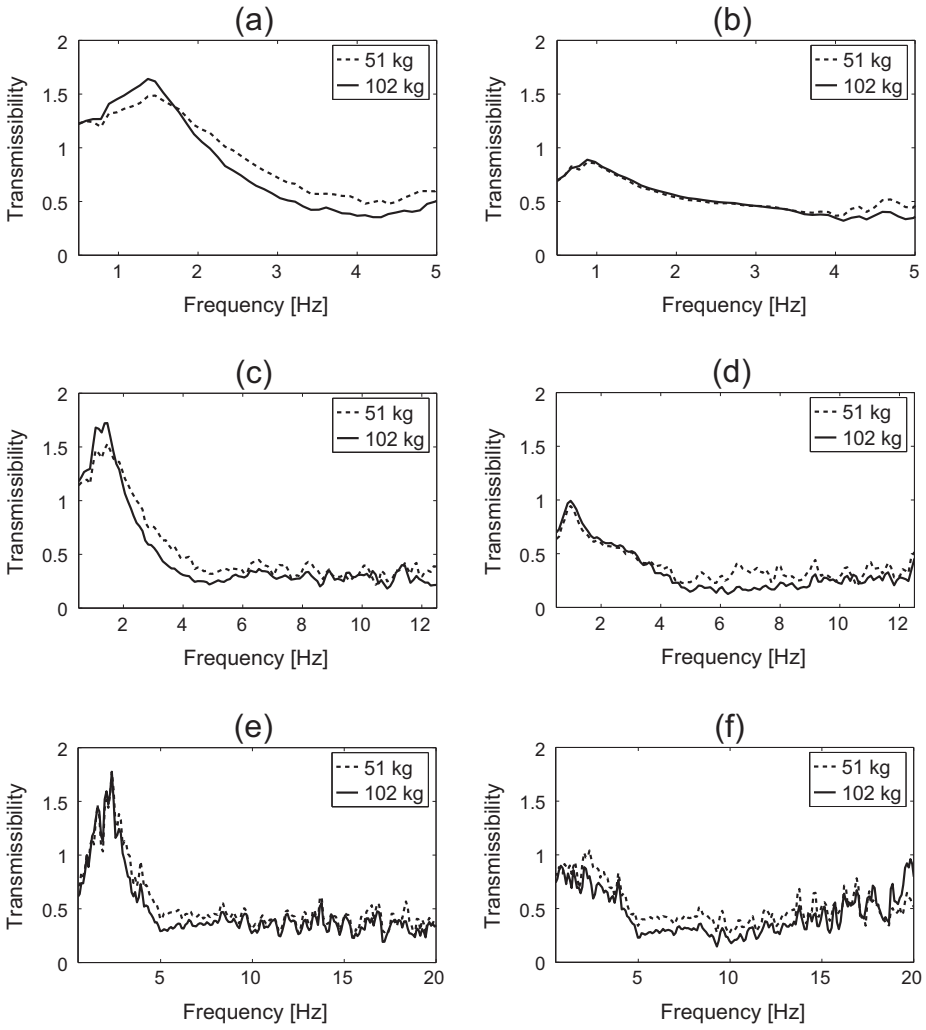

Fig. 12. Measured transmissibility functions of the passive seat suspension for various spectral classes of the excitation signal: EM3 (a), EM5 (c), EM6 (e) and measured transmissibility functions of the active seat suspension for various spectral classes of the excitation signal: EM3 (b), EM5 (d), EM6 (f).

As shown by the results obtained by means of numerical simulations (Fig. 6), the relative error of the recognised mass has the same behaviour for all excitation signals. The relative error is almost zero for low masses and around 130 kg, while underestimation between these masses and overestimation for higher masses is obtained. Such effect is caused by differences in mathematical modelling of the mass flow rate. In the following paper the Mietluk–Awtuszko function [24] is utilised to recognise the mass load, however a simulation model of the seat suspension has been built using a more general model of the mass flow rate given by St. Venant–Wantzel function [23]. The differences between these two models (cf. Fig. 7) clearly correspond to relative errors of the recognised mass load. Therefore, an appropriate selection of the model parameters has to be performed experimentally for a specific type of the proportional control valves.

4.7. Simulation results

The transmissibility curves of the simulated passive seat suspension for various mass loading 50 kg, 100 kg and 150 kg are presented in Fig. 8a, c, and e. As shown in this figure, the change of mass influences the dynamic behaviour of passive seat suspension. The suspension system loaded with the highest mass (150 kg) causes amplification of vibration at the resonance frequency (of about 1.3 Hz), but very good vibro-isolating properties are obtained for the higher frequencies (more than 4 Hz). The system loaded with a low mass (50 kg) has much lower amplification of vibration at resonance, but its vibration isolating properties at higher frequency range are poor. The dynamic behaviour of the active seat suspension (Fig. 8b, d, and f) loaded by a high mass (150 kg) and low mass (50 kg) are much closer to each other than the corresponding behaviour of the passive seat suspension. The active system is very efficient in reducing vibrations of the isolated body, as evidenced by significantly lower values of the SEAT factors. The comparison of particular SEAT factors and suspension travels, that are calculated for the input-spectral classes EM3, EM5 and EM5, are presented in Table 1. The simulation results showing the accelerations and the maximum relative displacements of the suspension system as a function of time are presented in Fig. 9.

For the purpose of the following paper, a comparison between the suggested control strategy and the already existing control is performed. In the authors' previous paper [22] a triple feedback loop control system of the active seat suspension responding to varying load mass has been analysed. Using a previously developed control system, the dynamic behaviour of the active seat suspension is investigated on the basis of numerical simulation. The comparison of both systems vibration damping performance is shown in Fig. 10. The results clearly present that the system robustness in response to a load mass change is higher in the case of the

Table 2
Measurement results of the active seat suspension for various spectral classes of the excitation signal and different human body mass.

Excitation signal	Human body mass (kg)	Passive		Active	
		SEAT factor	Suspension travel (mm)	SEAT factor	Suspension travel (mm)
EM3	51	0.972	74	0.527	78
	102	0.840	99	0.515	80
EM5	51	0.605	44	0.391	41
	102	0.461	62	0.346	43
EM6	51	0.471	8	0.431	9
	102	0.357	10	0.319	10

proposed active system than when it comes to the existing solution. This point is fundamental to show that the following paper improves the state of the art.

4.8. Measurement results

The dynamic behaviour of active system is also investigated experimentally using the test set-up presented in Fig. 11. This experimental set-up consists of a electro-hydraulic shaker which excites a vibration platform with the mounted seat. The seat is loaded by the light (51 kg) and heavy (102 kg) persons and each of the measurements takes 300 s. Based on the acceleration signals measured at the vibration platform and the seat cushion, the transmissibility functions for passive and active suspension systems are evaluated for various spectral classes of the excitation signals: EM3, EM5 and EM6. In Fig. 12 dynamical behaviour of the passive and active suspension systems is compared.

The results of experimental tests show (Fig. 12), that vibro-isolation properties of the active seat suspension are significantly improved relating to the passive system. The transmissibility functions obtained for the active system are lower than 1 in the whole frequency range, however the highest efficiency of the active control is achieved at resonance frequency for the passive seat (about 1.3 Hz). Harmful vibrations at this frequency are reduced of about 50% and also a desired system robustness in response to varying mass load is demonstrated (in the frequency range between 0.5 and 4 Hz). In this frequency range the air-flow effectively controls the air-spring force. At higher frequencies (more than 4 Hz) the shock-absorber force and the friction force are dominant. The particular SEAT factors and suspension travels measured for two different persons are presented in Table 2.

The simulation and experimental results shown in Tables 1 and 2 are similar in terms of the SEAT factor and the suspension travel. Regarding the passive system, the increase of load mass results not only in decreasing the SEAT factor but also in increasing the suspension travel. The SEAT factor for the active system is significantly lower than for the passive system. The reduction of the suspension travel is also observed for high suspension load mass. Better vibration control properties of the active system in respect of the passive one and better robustness to varying load mass are demonstrated by simulation and experimental studies.

5. Conclusions

The active control proposed in this paper significantly improves a performance of the seat suspension. The calculated reverse model of the pneumatic spring together with the primary controller efficiently controls the active seat suspension dynamic behaviour. Moreover, the elaborated controller with adaptive mass recognising enhances the desired system robustness in response to varying mass loading. In order to achieve the desired vibro-isolation properties of the active seat suspension, an appropriate selection of the constraint value imposed on the suspension travel is required. For the chosen value, the controller settings can be evaluated and their values define the vibration damping effectiveness of the seat suspension.

Acknowledgements

The following work is a part of the research project "Methods and procedures of selecting vibro-isolation properties of vibration reduction systems" founded by the National Science Center of Poland under the contract No. UMO-2013/11/B/ST8/03881. We would like to thank Isringhausen GMBH and CO. KG for the assistance in the experimental research.

Appendix A. Parameter values used by the pneumatic spring model

Effective area of the air-spring (A_{ef})	7.164×10^{-3} m^2
Gravity constant (g)	9.81 m/s^2
Static gain of the inlet valve (k_I)	1.28×10^{-6} m^2/V
Static gain of the outlet valve (k_E)	1.28×10^{-6} m^2/V
Air pressure of the power supply (p_z)	9×10^5 Pa
Atmospheric pressure (p_a)	1×10^5 Pa
Actuating time of the inlet valve (t_I)	0.01 s
Actuating time of the outlet valve (t_E)	0.01 s
Air temperature (T)	293 K
Maximum voltage of the control valve (u_{max})	10 V
Parameter of the Mietluk–Awtuszko function (α)	1.13
Reduction ratio of active force (δ_s)	0.35
Adiabatic coefficient (κ)	1.4

References

[1] Thompson AG. Optimum damping in a randomly excited non-linear suspension. Proc Inst Mech Eng 1969;184:169–84.
[2] Karnopp D. Analytical results for optimum actively damped suspensions under random excitation. ASME J Vib Acoust Stress Reliab Des 1989;111:278–83.
[3] Crolla DA. Semi-active suspension control for a full vehicle model. SAE technical paper series 911904; 1992. p. 45–51.
[4] Goodall RM, Kortüm W. Active control in ground transportation – review of the state-of-the-art and future potential. Veh Syst Dyn 1983;12:225–57.
[5] Hrovat D. Optimal active suspensions for 3d vehicle models. In: Proc of the American control conference. Arizona, USA, vol. 2; 1991. p. 1534–41.
[6] Stein GJ. Results of investigation of an electro-pneumatic active vibration control system. Proc Inst Mech Eng Part D: J Autom Eng 1995;209:227–34.
[7] Maciejewski I. Control system design of active seat suspensions. J Sound Vib 2012;331:1291–309.
[8] Maciejewski I, Krzyzynski T. Control design of semi-active seat suspension. J Theor Appl Mech 2011;49(4):1151–68.
[9] Choi SB, Lee HK, Chang EG. Field test results of a semi-active ER suspension system associated with skyhook controller. Mechatronics 2001;11:345–53.
[10] Bouazara M, Richard MJ, Rakheja S. Safety and comfort analysis of a 3-D vehicle model with optimal non-linear active seat suspension. J Terramech 2006;43:97118.
[11] Ksiazek MA, Ziemianski D. Optimal driver seat suspension for a hybrid model of sitting human body. J Terramech 2012;49:255–61.
[12] Sun W, Li J, Zhao Y, Gao H. Vibration control for active seat suspension systems via dynamic output feedback with limited frequency characteristic. Mechatronics 2011;21:250–60.
[13] Zhang H, Wang R, Wang J, Shi Y. Robust finite frequency H-inf static-output-feedback control with application to vibration active control of structural systems. Mechatronics 2014;24(6):354–66.
[14] Gao H, Lam J, Wang Ch. Multi-objective control of vehicle active suspension systems via load-dependent controllers. J Sound Vib 2006;290:654–75.
[15] Chen P-Ch, Huang A-Ch. Adaptive sliding control of non-autonomous active suspension systems with time-varying loadings. J Sound Vib 2005;282:1119–35.

[16] Maciejewski I. Load-dependent controller of the active seat suspension with adaptive mass recognizing. Acta Mech Autom 2012;6(2):66–70.
[17] International Organization for Standarization. Earth-moving machinery – laboratory evaluation of operator seat vibration. ISO 7096, Geneva; 2000.
[18] Griffin MJ. Handbook of human vibration. London: Elsevier Academic Press; 1996.
[19] International Organization for Standarization. Mechanical vibration and shock – evaluation of human exposure to whole-body vibration. ISO 2631, Geneva; 1997.
[20] Maciejewski I, Meyer L, Krzyzynski T. Modelling and multi-criteria optimisation of passive seat suspension vibro-isolating properties. J Sound Vib 2009;324:520–38.
[21] Fialho I, Balas GJ. Road adaptive active suspension design using linear parameter-varying gain-scheduling. IEEE Trans Control Syst Technol 2002; 10(1):43–54.
[22] Maciejewski I, Meyer L, Krzyzynski T. The vibration damping effectiveness of an active seat suspension system and its robustness to varying mass loading. J Sound Vib 2010;329:3898–914.
[23] Beater P. Pneumatic drives, system design, modelling and control. Berlin Heidelberg: Springer-Verlag; 2007.
[24] Kiczkowiak T. Algorithms and models applied in the design of pneumatic driving systems. Koszalin: Publishing House of Koszalin University of Technology; 2005 [in Polish].